Available online at www.sciencedirect.com
SCIENCE DIRECT
Journal of Catalysis 240 (2006) 8–17
JOURNAL OF CATALYSIS
www.elsevier.com/locate/jcat

The kinetics of vapour-phase ammoxidation of 2,6-dichlorotoluene over VPO catalyst

N. Dropka, V. Narayana Kalevaru, A. Martin *, D. Linke, B. Lücke

Institute für Angewandte Chemie Berlin-Adlershof e.V. [1]*, Richard-Willstätter-Str. 12, D-12489 Berlin, Germany*

Received 20 October 2005; revised 27 February 2006; accepted 27 February 2006

Available online 30 March 2006

Abstract

The kinetics of the vapour-phase ammoxidation of 2,6-dichlorotoluene (DCT) to 2,6-dichlorobenzonitrile (DCBN) over a vanadium phosphorus oxide (VPO) catalyst was investigated. In this paper, the main focus is on developing a mathematical model to describe the reaction kinetics of ammoxidation of DCT in a nonisothermal fixed-bed lab-scale reactor. The effect on catalytic performance of various operating parameters, including reaction temperature and contact time, as well as of DCT, NH_3, O_2, and H_2O partial pressures, were studied. The experimental kinetic data obtained under nonisothermal conditions were correlated by the rate equations based on the Langmuir–Hinshelwood mechanism. All of the possible routes of reaction scheme were considered. Finally, the derived kinetic model was validated by comparing experimental results obtained in up-scaled experiments from a mini-plant with that of simulated results. The simulated values of various parameters, including the conversions of DCT and O_2 and even the yields of DCBN and CO_x, agree well with those of experimentally measured values.

Keywords: Promoted VPO catalyst; Ammoxidation; 2,6-Dichlorotoluene; Kinetic modelling; Reaction scheme; Mini-plant experiments; Simulation and validation

1. Introduction

Heterogeneously catalysed ammoxidation enables the conversion of olefins and alkyl aromatics as well as hetero aromatics in the presence of oxygen and ammonia to the corresponding nitriles [1]. The most commercially important ammoxidation process is that developed by Sohio for the production of acrylonitrile from propylene [2]. Vapour-phase ammoxidation of alkyl aromatics and hetero aromatics is gaining considerable importance as a commercial method for producing various industrially important nitriles [1,3–5]. These reactions have been the subject of many industrial applications and patents [6–10]. Despite this growing interest, however, few scientific studies have been conducted on the reaction kinetics of various aromatics. Several reaction mechanisms have been proposed, but the actual mechanism of alkyl aromatic ammoxidation remains unclear. The reaction pathway likely depends on both the catalyst and the reaction conditions, and hence different pathways may be present. In addition, investigators have found it difficult to isolate some of the highly reactive intermediates to confirm the proposed mechanisms.

In particular, ammoxidation of 2,6-dichlorotoluene (DCT) is an industrially important reaction for producing 2,6-dichlorobenzonitrile (DCBN) in a single step. The desired product (DCBN) is basically a kind of herbicide and also a useful intermediate in the preparation of a series of highly efficient pesticides (hormone-type pesticides). DCBN can also be used in the preparation of various special kinds of engineering plastics with high thermal resistance. The ammoxidation of DCT to DCBN to obtain higher conversions and yields compared with those of other alkyl aromatics is a very difficult and challenging process. Because the methyl group to be oxidised (ammoxidised) is less active due to restricted accessibility (i.e., steric hindrance) owing to the presence of two bulky chloride atoms on both the ortho positions of the methyl group, as shown in Scheme 1.

Although numerous articles are available on ammoxidation reactions in general, only a few papers have been pub-

* Corresponding author.
E-mail address: a.martin@aca-berlin.de (A. Martin).

[1] A member of the EU-funded Coordination Action of Nanostructured Catalytic Oxide Research and Development in Europe (CONCORDE).

0021-9517/$ – see front matter
doi:10.1016/j.jcat.2006.02.025

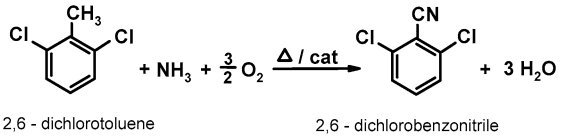

Scheme 1.

lished in the open literature specifically on the ammoxidation of dichlorotoluenes and DCT [11–13]. Our own investigations were carried out using vanadium phosphates (VPO) as catalysts [11,12], whereas the article of Qiong et al. [13] does not mention the catalyst composition. Furthermore, most of the data published on the ammoxidation of DCT are guarded by various patents [14–17]. Therefore, there is much opportunity for developing improved catalyst compositions, along with a great need for research on the mechanism and other aspects of ammoxidation of DCT due to its significant industrial importance and the eco-friendly nature. To date, no studies of the reaction kinetics of catalytic ammoxidation of DCT have been published. Consequently, the present study is an attempt to develop greater insight into the kinetics of this reaction by estimating parameters that allow simulation of the reaction in a wide range of conditions.

2. Experimental

2.1. Catalyst preparation

Catalyst preparation involves three steps: (i) preparation of bulk VPO precursor in an organic medium, (ii) preparation of bulk-promoted VPO solid with suitable additive (i.e., Cr) by an impregnation technique, and (iii) preparation of TiO_2 (anatase)-supported VPCrO catalyst by a solid–solid wetting method.

2.1.1. Preparation of the bulk VPO precursor [i.e., $VOHPO_4{\cdot}0.5H_2O$ (P/V = 0.95)]

A 52.5-g sample of V_2O_5 (UH: 2862; Gesellschaft für Elektrochemie, Nürnberg) was suspended in a mixture of 315 ml of 2-butanol (purity >99%, Merck) and 210 ml of benzyl alcohol (purity >99%, Merck) at room temperature. The suspension was stirred continuously under reflux at 393 K for 3 h, then cooled to room temperature and kept under stirring at room temperature overnight. Then 63.23 g of 85% *o*-H_3PO_4 was slowly added, and the solution was again heated and maintained under reflux at 393 K with constant stirring for 2 h. The resulting slurry was cooled to room temperature, filtered, and washed with ethyl alcohol. The precursor thus obtained was oven dried at 393 K for 24 h.

2.1.2. Preparation of bulk-promoted VPO precursor (P/V = 0.95; M/V = 0.05)

The required amount of chromium source [$Cr(NO_3)_3{\cdot}9H_2O$] was dissolved in ca. 40 ml of ethanol. The solution was heated on a water bath for some minutes, and the uncalcined $VOHPO_4{\cdot}0.5H_2O$ precursor (25 g) was slowly added in powder form to the above solution. Then the slurry was evaporated to dryness on a water bath/hot plate. The resulting solid was dried in an oven at 393 K for 16 h.

2.1.3. Preparation of (supported and promoted) 25 wt% VPO catalyst

Subsequently, 15 g of carrier [TiO_2 (anatase)] is placed in a porcelain mortar, and 5 g of amount of bulk-promoted VPCrO powder was added. Both solids were present in powder form. The components were thoroughly mixed manually for about 15 min until a uniform colour of the mixture was attained.

Finally, the catalyst was shaped and calcined at 723 K for 3 h. A calcining atmosphere under weak oxidising strength, composed of 0.5% O_2/N_2, was used. This promoted catalyst [i.e., VPCrO/TiO_2 (anatase)] had a P/V ratio of 0.95, a Cr/V (atomic ratio) of 0.05, and a VPCrO loading of 25 wt%.

For lab-scale experiments, 2-cm-diameter tablets were pressed at 15 bar, calcined, and crushed to smaller particles. After sieving, a fraction with diameters ranging from 1 to 1.25 mm was used for the tests. The mini-plant runs were carried using a catalyst from the same batch that was industrially shaped by a tableting machine to 5 × 3.5 mm tablets using 5% graphite as a sliding additive. The tablets were calcined in the same way as described above.

2.2. Catalytic tests

2.2.1. Lab-scale experiments

In general, tests for evaluation of catalytic performance and measurements under kinetic regime were carried out in a fixed-bed tubular glass reactor with an inner diameter of 12.3 mm and a reactor length of 135 mm placed into an aluminium block furnace. A thermocouple was placed in the centre of the reactor to measure the temperature profile along the catalyst bed. The catalyst was diluted with glass beads at a ratio of 1:(1–10) with an intention to achieve isothermicity. However, such isothermicity could not be achieved because of the highly exothermic nature of the reaction; on the other hand, higher dilutions were not possible due to the limitations of the experimental setup. In other words, the highest dilution possible was applied. A fraction of catalyst particles with diameters as described above was loaded into the reactor. Experiments were performed at atmospheric pressure at four temperatures (630, 652, 675, and 700 K). Different residence times were established by varying the weight of the catalyst in a range of 0.6–6 g with a fixed gas flow rate of 150 ml_{STP}/min. To analyse different possible influences on the kinetics, the concentrations of the components of the reaction mixture, such as DCT (purity >98%, Fluka, Germany), O_2 (purity >99.995%, Messer), NH_3 (purity >99.98%, Messer), and H_2O, were varied while keeping the rest of the gas composition constant (reference composition: $DCT:O_2:NH_3:H_2O:Ne = 2.4:13:10:20:54.6$).

Ne was used as a diluent gas because of better GC separation from oxygen compared with other inert gases (He, Ar) and also because N_2 was a product of ammonia oxidation and not an inert in this reaction. Based on earlier results, adding water to the feed was found to enhance the catalytic performance of the catalysts. It is also known from the literature that the addition of water changes the ratio of Lewis to Brønsted acid sites, moderates reaction temperature, reduces total oxidation, and affects the extent of surface hydroxylation.

The liquid feed components (DCT and H_2O) were pumped using two separate HPLC pumps. The gaseous reactants were dosed by mass flow controllers (MFC). Pure O_2 and Ne were used separately from two different compressed gas cylinders. The liquids were vaporised, mixed with the reaction gases, and fed to the catalyst bed after preheating. The reactor outlet stream may contain solids (DCBN, NH_4Cl), liquids (DCT, H_2O) and gaseous components; therefore, the liquids and solids (after dissolving in ethanol) were analysed off-line by a gas chromatograph equipped with a flame ionization detector module, whereas the gaseous components were analysed on-line by a micro-gas chromatograph equipped with a thermal conductivity detector using two separate columns. Estimation of O_2, N_2, CO, and Ne gases was carried out using a MS-5A column, and estimation of CO_2 was done with a Poraplot-Q column.

2.2.2. Mini-plant experiments

The mini-plant was equipped with a stainless steel fixed-bed reactor, MFCs and various pumps for feeding the reactants, on line-analysis (GC), cooling, and separation units for separating liquid products from gaseous mixture. The separation of liquid and gaseous products took place in a cooler; flash in situ cooling using an additional cooling stream was also applied. The experiments in the mini-plant were carried out in the aforementioned reactor (i.d., 31.7 mm; length, 175 mm) at atmospheric pressure using 20.8 g of 25% $VPCrO/TiO_2$ catalyst (5×3.5 mm tablets) diluted with glass beads in a ratio of 1:5. The catalyst was previously up-scaled, as described above. The flow rates of gaseous feed components were measured using mass flow controllers. The liquid feeds, like DCT and water, were dosed separately using HPLC pumps. The gaseous stream was preheated, then introduced to the reactor along with vaporised liquid feed (DCT) and water. All subsequent transfer lines were heated to 633–673 K to avoid the condensation and adsorption of product components, mainly to prevent deposition of NH_4Cl. The separation of product stream coming out of the reactor was done by cooling and quenching of the hot gaseous stream by sour water (diluted sulphuric acid/organic solution) in an absorption column. Subsequently, the products and unconverted reactants were estimated by GC.

3. Results and discussion

3.1. Evaluation of the catalytic performance of the 25 wt% $VPCrO/TiO_2$ catalyst in a lab-scale reactor

The experimental results showed a nonisothermal catalyst bed especially at higher reaction temperatures, due to the exothermic nature of the reaction. Axial temperature gradients up to 20–30 K were observed, depending on reaction conditions applied. Therefore, we discuss the influence of partial pressures of different components only at 630 K, where the behaviour was nearly isothermal. We discuss the behaviour at higher temperatures qualitatively, to confirm the conclusions drawn from the results at lower temperatures. The results at all temperatures were used in the determination of kinetic parameters. Each experiment was repeated several times, and the results were found to be quite reproducible. Carbon balances >95% were obtained for all experiments reported here; therefore, the formation of other byproducts is not very significant.

In the lab-scale catalytic experiments, the 25% $VPCrO/TiO_2$ (anatase) catalyst allowed yields of up to 82% at a conversion of 91% (DCBN selectivity up to ca. 90%). During all experiments, only trace amounts of HCN, NO_x, and $C_6H_4Cl_2$ were found, and these were excluded from the reaction scheme. The experimental data also showed that DCBN was stable even at high temperatures; its yield continuously increased in the entire range of temperatures investigated (Fig. 1). The dependence of conversions of DCT and O_2 and yields of products from the modified residence time at $T = 630$ K are shown in Fig. 2.

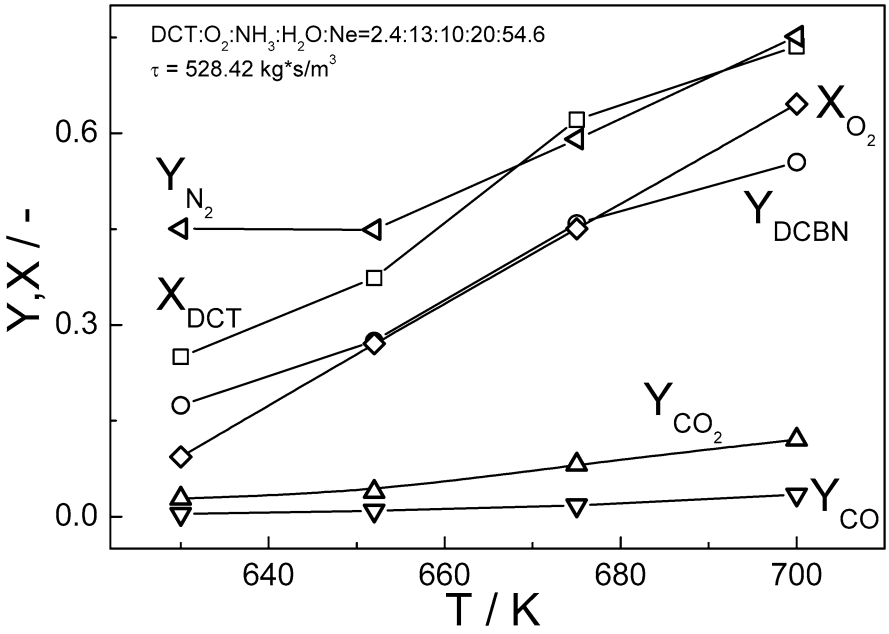

Fig. 1. Influence of temperature on conversion of DCT and O_2 as well as yields of DCBN, CO_x and N_2.

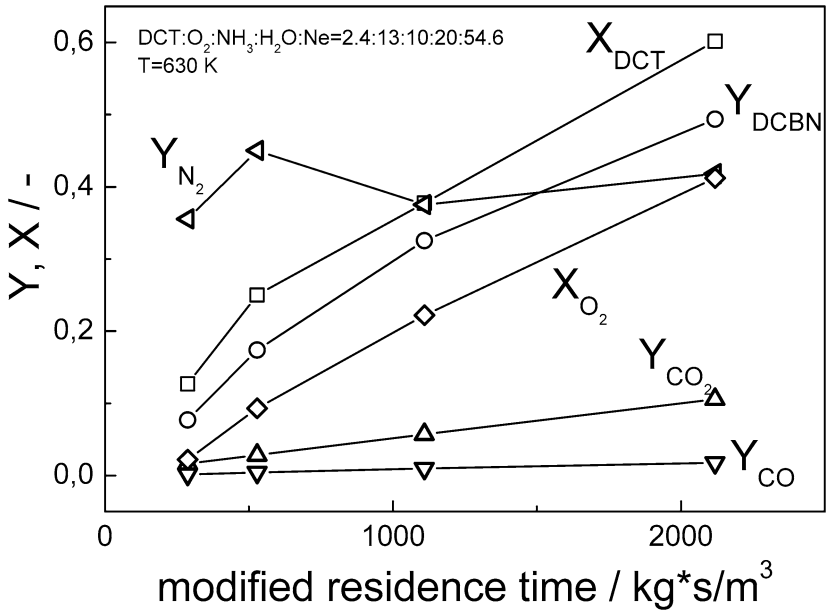

Fig. 2. Conversion of DCT and O_2 as well as yields of DCBN, CO_x and N_2 as a function of modified residence time.

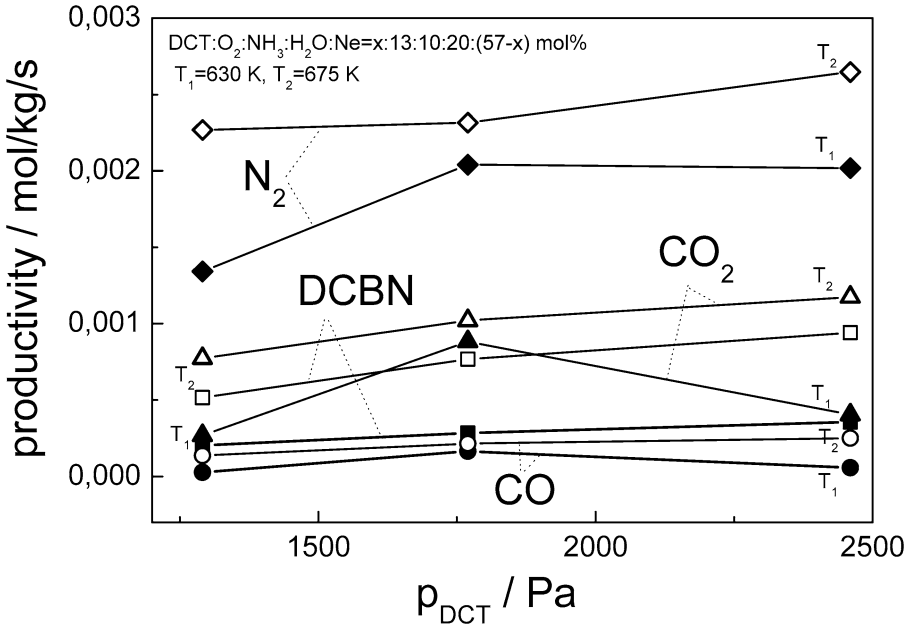

Fig. 3. Influence of DCT partial pressure on the yields of DCBN, CO_x and N_2.

The effect of varying the DCT concentration in the feed (keeping the O_2, NH_3, and H_2O concentrations constant) is shown in Fig. 3. The yields of DCBN, CO, CO_2, and N_2 as a function of partial pressure of DCT in a range of 1.3–2.4 kPa showed an inhibiting effect of DCT on the rates of CO_x formation. The fact that DCT had no effect on the formation of N_2 from NH_3 could be direct evidence of the existence of another active site for ammonia oxidation. The increased N_2 yield with increasing DCT partial pressure may be the result of the inhibited rate of formation of carbon species, leaving the unused O_2 that takes part in ammonia combustion. If there were only one active site with competitive adsorption of DCT and NH_3, then N_2 yield should drop with an increase in DCT. In general, all ammoxidation reactions of aromatics are known for their competitive adsorption between aromatics and NH_3; therefore, it can be concluded that at least two active sites exist: one for ammonia oxidation and another one for selective and nonselective DCT oxidation. The differing intensity of inhibition of CO_x and DCBN rates of formation by DCT gives rise to an assumption of the possible existence of a third active site, for example, different active sites for CO_x formation and DCBN formation. Similar behaviour was reported for TiO_2(B)-supported vanadium oxide catalyst in the ammoxidation of toluene [18].

The influence of oxygen on the rates of formation of products is illustrated in Fig. 4. The oxygen partial pressure was varied in a range of 6–13.5 kPa, in excess with respect to the

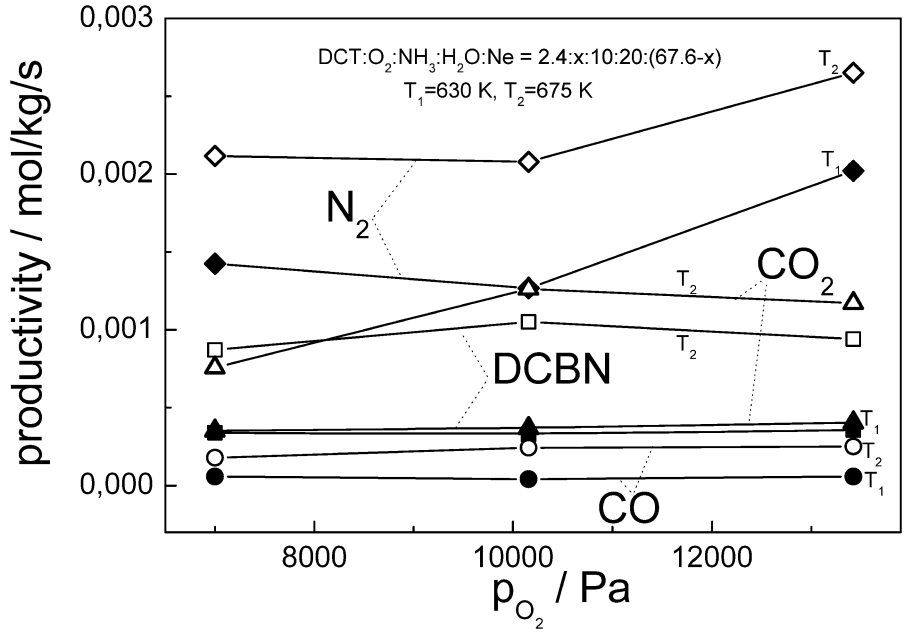

Fig. 4. Influence of oxygen partial pressure on the yields of DCBN, CO_x and N_2.

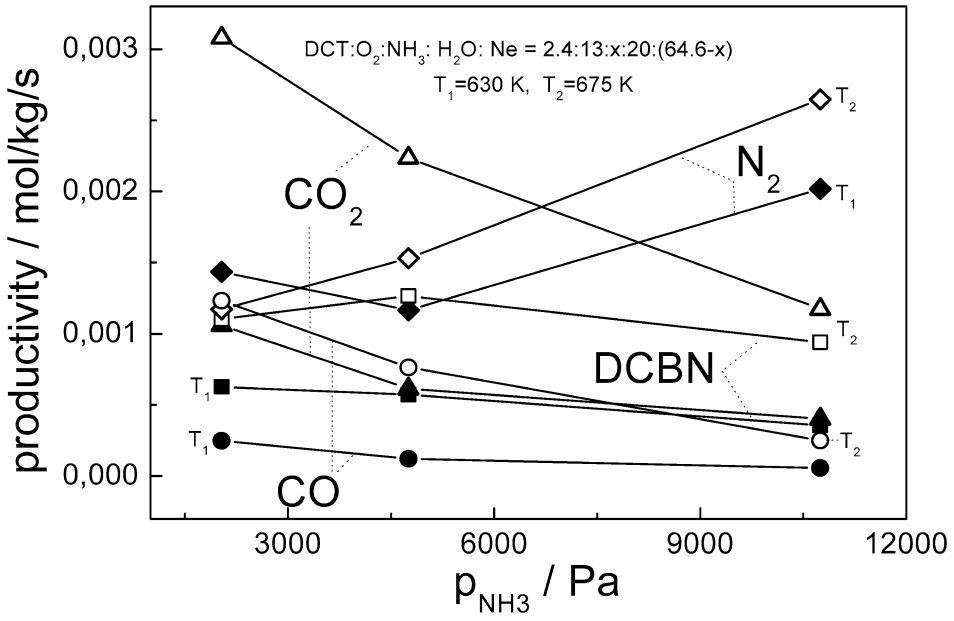

Fig. 5. Influence of ammonia partial pressure on the yields of DCBN, CO_x and N_2.

theoretical stoichiometric amounts. The dependence of rates of DCBN, CO, and CO_2 formation at the lowest temperature (630 K) on the amount of oxygen was found to be practically zero. This was not the case for the rate of ammonia combustion, however; N_2 formation increased at higher O_2 concentrations. At $T = 673$ K, it seems that the rate of CO_2 formation was also influenced by O_2, but because of the nonisothermicity of these experiments, this conclusion can be considered only speculative.

NH_3 partial pressure exhibited an interesting influence on the rate of formation of products (Fig. 5). Ammonia was varied in a range of 2.0–10.7 kPa. Its inhibiting behaviour on the formation of all carbon oxides can be seen in the entire range of concentrations. When ammonia concentration was decreased to low values, CO_2 increased significantly, at a rate tending to values corresponding to DCT oxidation (with formation of high amounts of carbon dioxide). The formation of DCBN showed a negative order at higher ammonia concentrations. At ammonia concentrations below the formal stoichiometric amount, the effect of ammonia on DCBN formation seemed to be positive (pronounced at 675 K), confirming the results of Simon and Germain [19] and Cavalli et al. [20] that a certain percentage of ammonia stabilises the initial product of feed (methyl aromatic) activation, probably an adsorbed radical species, inhibiting its oxidation to CO_2. Our own investigations have shown that ammonia can block acidic sites (e.g., Brønsted acid sites),

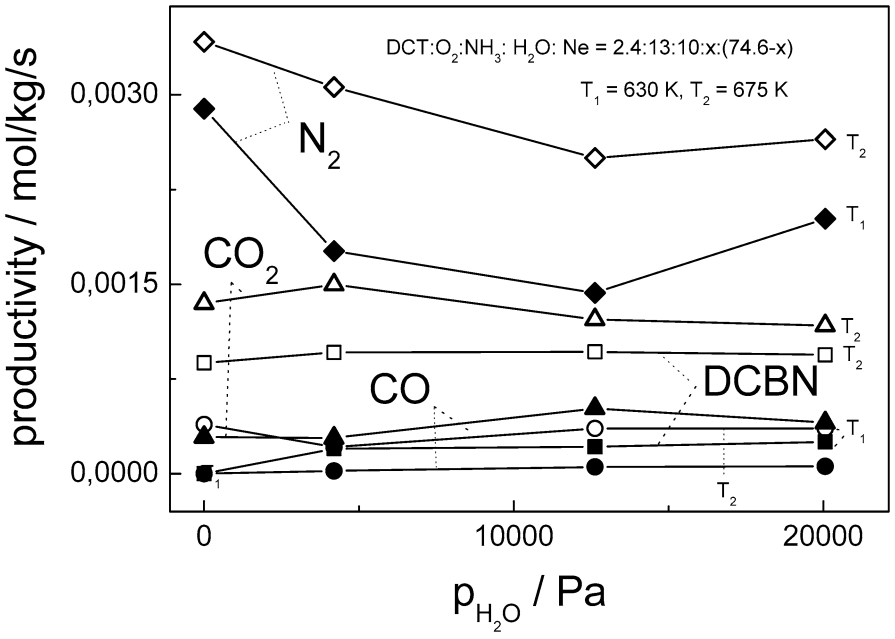

Fig. 6. Influence of water partial pressure on the yields of DCBN, CO_x and N_2.

which may be responsible for stronger adsorption of the partial oxidised intermediates [21]. The formation of N_2 showed a positive dependence on ammonia concentration.

The effect of H_2O partial pressure on the rates of formation of all products is shown in Fig. 6. An inhibiting effect of H_2O on N_2 formation was found, in agreement with the generally accepted role of water in inhibiting ammonia oxidation under ammoxidation reaction conditions. At higher levels of dilution with water at 630 K, ammonia oxidation appeared to be enhanced. The precise reason for this effect remains unclear, and further studies are needed. Only a weak negative effect on formation of carbon species at higher reaction temperature (675 K) was observed.

3.2. Kinetic modelling

3.2.1. Methodology

Because most of the kinetic data demonstrated nonisothermicity, it was necessary to apply a nonisothermal reactor model for evaluation of such kinetic data. A steady-state pseudo-homogeneous fixed-bed tubular reactor model with negligible axial and radial diffusion was chosen. Corresponding differential and algebraic equations describe this model:

$$\frac{\partial F_i}{\partial V} = \rho_B R_i, \tag{1}$$

$$F = \sum_{i=1}^{N} F_i, \tag{2}$$

$$W\frac{\partial \hat{H}}{\partial V} = U\alpha(T_a - T) \tag{3}$$

and

$$W\hat{C}_p\frac{\partial T}{\partial V} = U\alpha(T_a - T) - \rho_B\sum_{i=1}^{N}\bar{H}_i R_i, \tag{4}$$

with auxiliary equations

$$R_i = R_i(C, T, P), \quad C_i = \frac{F_i}{F}\frac{\rho}{M_w}, \quad \rho = \frac{PM_w}{zRT}, \quad \alpha = \frac{4}{D_t},$$

where C is molar concentration (mol/m^3), D is diameter (m), F is molar flow (kmol/s), H is enthalpy of reaction (kJ/kmol), M is molar mass (kmol/kg), P is pressure (kPa), R is reaction rate per mass of the catalyst (kmol/(kg s)), T is temperature (K), U is overall heat transfer coefficient (kJ/(m^2 h K)), V is volume (m^3), W is mass flow (kg/s), α is area of heat transfer per reaction volume (1/m), and ρ is density (kg/m^3).

In the experimental setup applied in the kinetic experiments, the pressure drop along the reactor can be considered negligible. Because the temperature profile along the reactor was measured, we could have applied van Damme's approach [22] and skipped solving the energy equation, but we decided to solve these coupled differential equations that completely describe the system and to use the measured T profile along the reactor as an accuracy test.

We solved this nonlinear initial value problem involving a system of differential and algebraic equations numerically using a predictor-corrector algorithm (Athena Visual Workbench 8.3). The estimation of the kinetic parameters resulted from the solution of a quadratic minimisation problem applying a modified Gauss–Jordan algorithm within a user-defined feasible region. The objective function, a weighted sum of squared residuals for molar flows of DCT, DCBN, CO, CO_2, O_2, and N_2 and for outlet temperature, was expanded as a quadratic function of the parameters around the initial parameter values of the current iteration.

3.2.2. Reaction schemes and reaction models

On the basis of experimental results, we can assume that the general network of the reaction (Table 1) consists of the

Table 1
Reaction scheme (reaction enthalpies given at $T = 673$ K)

1	$C_6H_3Cl_2CH_3 + NH_3 + 1.5O_2 \rightarrow C_6H_3Cl_2CN + 3H_2O$	$\Delta H_1 = -517$ kJ/mol
2	$C_6H_3Cl_2CH_3 + 8O_2 \rightarrow 7CO_2 + 2H_2O + 2HCl$	$\Delta H_2 = -3411$ kJ/mol
3	$C_6H_3Cl_2CH_3 + 4.5O_2 \rightarrow 7CO + 2H_2O + 2HCl$	$\Delta H_3 = -1430$ kJ/mol
4	$2NH_3 + 1.5O_2 \rightarrow 3H_2O + N_2$	$\Delta H_4 = -316$ kJ/mol
5	$NH_3 + HCl \leftrightarrow NH_4Cl$	$\Delta H_5 = -170.5$ kJ/mol

primary ammoxidation of DCT (step 1) and combustion reactions (steps 2 and 3). Ammonia combustion was presented in step 4. HCl as a possible product could not be measured in the outlet stream, because the reaction stream was analysed at the ambient temperature where the equilibrium of reaction 5 (Table 1) was shifted irreversibly to the NH_4Cl direction. This reaction step becomes important in the reactor simulation if the postreaction zone is included in a system under consideration.

In interpreting the reaction kinetics based on the experimental data, a treatment based on the Langmuir–Hinshelwood mechanism, in which the rate-controlling step in the process is the chemical reaction on the surface of the catalyst, was used. In view of experimental findings (e.g., analysis of the concentration's effects on the rates of product formation), the following kinetic model/rates r_i were tested (for the reaction network shown in Table 1):

$$r_i = \frac{k_i p_{\mathrm{DCT}}}{1 + K_{\mathrm{DCT}} p_{\mathrm{DCT}} + K_{\mathrm{NH_3}} p_{\mathrm{NH_3}}}, \quad i = 1, \ldots, 3,$$

$$r_4 = \frac{k_4 p_{\mathrm{NH_3}} p_{\mathrm{O_2}}}{1 + K^*_{\mathrm{NH_3}} p_{\mathrm{NH_3}} + K_{\mathrm{H_2O}} p_{\mathrm{H_2O}}},$$

$$r_5 = k_5 p_{\mathrm{NH_3}} p_{\mathrm{HCl}} - \frac{k_5}{K} p_{\mathrm{NH_4Cl}},$$

$$K = \frac{p_{\mathrm{NH_4Cl}}}{p_{\mathrm{NH_3}} p_{\mathrm{HCl}}}.$$

In this model, all reactions are taking place at two active sites: one site for ammonia oxidation and one site for selective and nonselective DCT oxidation. The formation of DCBN and CO_x depend on DCT partial pressure according to Langmuir–Hinshelwood dependence and are independent of oxygen partial pressure; that is, the reaction proceeds via direct participation of lattice O atoms according to the Mars–van Krevelen mechanism [23] for oxidation of aromatics on V_2O_5. A similar mechanism has also been presented for the ammoxidation of various alkyl aromatics [24,25].

The inhibiting effect of ammonia on the conversion of DCT was attributed to its competition with DCT for the similar active sites. Ammonia oxidation depends on ammonia and oxygen partial pressures and is inhibited by H_2O and NH_3 adsorption. Ammonia is oxidised by gas-phase oxygen, whereas DCBN is formed in oxidation by lattice oxygen. These different oxygen types in a model exhibit differing influences of oxygen on the rate of formation of carbon-containing compounds and N_2. No adsorbed DCT in the rate expression for NH_3 oxidation was drawn from the fact that N_2 formation was accelerated by higher DCT partial pressures. It is possible if DCT is inhibiting the formation of C-species, leaving more unused O_2 that can increase the rate of N_2 formation. Different roles of H_2O in steps 1 and 2 and in step 3 (see Table 1) resulted from the fact that N_2 formation is affected differently by increased H_2O partial pressure than the carbon species. Along with this simple model with two active sites, an additional model with three active sites (i.e., the separate active sites for DCT and CO_x formation) was studied.

Table 2
Kinetic parameters for model with two active sites

Parameter	Value
k_1 (10^7 mol/(kg s Pa))$_{630\,\mathrm{K}}$	9.85
k_2 (10^7 mol/(kg s Pa))$_{630\,\mathrm{K}}$	2.22
k_3 (10^8 mol/(kg s Pa))$_{630\,\mathrm{K}}$	6.39
k_4 (10^{10} mol/(kg s Pa^2))$_{630\,\mathrm{K}}$	7.37
k_5 (10^{20} mol/(kg s Pa^2))$_{630\,\mathrm{K}}$	1.00
K_{DCT} (10^4 Pa^{-1})$_{630\,\mathrm{K}}$	4.99
$K_{\mathrm{NH_3}}$ (10^4 Pa^{-1})$_{630\,\mathrm{K}}$	4.63
$K_{\mathrm{H_2O}}$ (10^3 Pa^{-1})$_{630\,\mathrm{K}}$	1.00
$K_{\mathrm{NH_3}}$[a] (10^3 Pa^{-1})$_{630\,\mathrm{K}}$	3.30
$E_{\mathrm{A_1}}$ (kJ/mol)	56.9
$E_{\mathrm{A_2}}$ (kJ/mol)	50.2
$E_{\mathrm{A_3}}$ (kJ/mol)	40.0
$E_{\mathrm{A_4}}$ (kJ/mol)	50.7
$E_{\mathrm{A_5}}$ (kJ/mol)	40.0
ΔH_{DCT} (kJ/mol)	−29.3
$\Delta H_{\mathrm{NH_3}}$ (kJ/mol)	−100.0
$\Delta H_{\mathrm{H_2O}}$ (kJ/mol)	−39.4
$\Delta H_{\mathrm{NH_3}}$[a] (kJ/mol)	−52.7

[a] Differentiation between adsorption constant for NH_3 in reaction steps 1–3 and step 4 (see Table 1).

3.3. Results of kinetic evaluation

Parity plots for molar fractions of DCT, DCBN, CO_x, O_2 and N_2 for model with the two active sites are given in Fig. 7. The corresponding kinetic parameters are summarised in Table 2. Reaction 5 (see Table 1) can be considered negligible under the reaction conditions examined, with the rate of forward reaction several orders of magnitude slower than the other reaction steps. The corresponding equilibrium constant is $K_{674\,\mathrm{K}} = 0.939$.

The rate of DCBN formation is one order of magnitude faster than the rates of CO and CO_2 formation (k_1 compared with k_2 and k_3). The competitive reaction to DCBN formation is the ammonia oxidation to N_2. This significant side reaction in other ammoxidation processes can consume >50% of NH_3 at the higher temperatures [2], depleting O_2 from the feed and hence inhibiting the desired ammoxidation reaction to a greater extent. The weaker adsorption of H_2O compared with NH_3 is not surprising, because water is a much weaker Lewis base than NH_3.

The results for the model with two active sites showed a slightly better fit than the model with three active sites (−5.34E3 compared with −5.37E3 as a value of objective function). Despite only a small difference in residual of these two models, the model with two active sites takes priority, being simpler and bearing in mind published results concerning kinetic studies of the ammoxidation of alkyl aromatics over

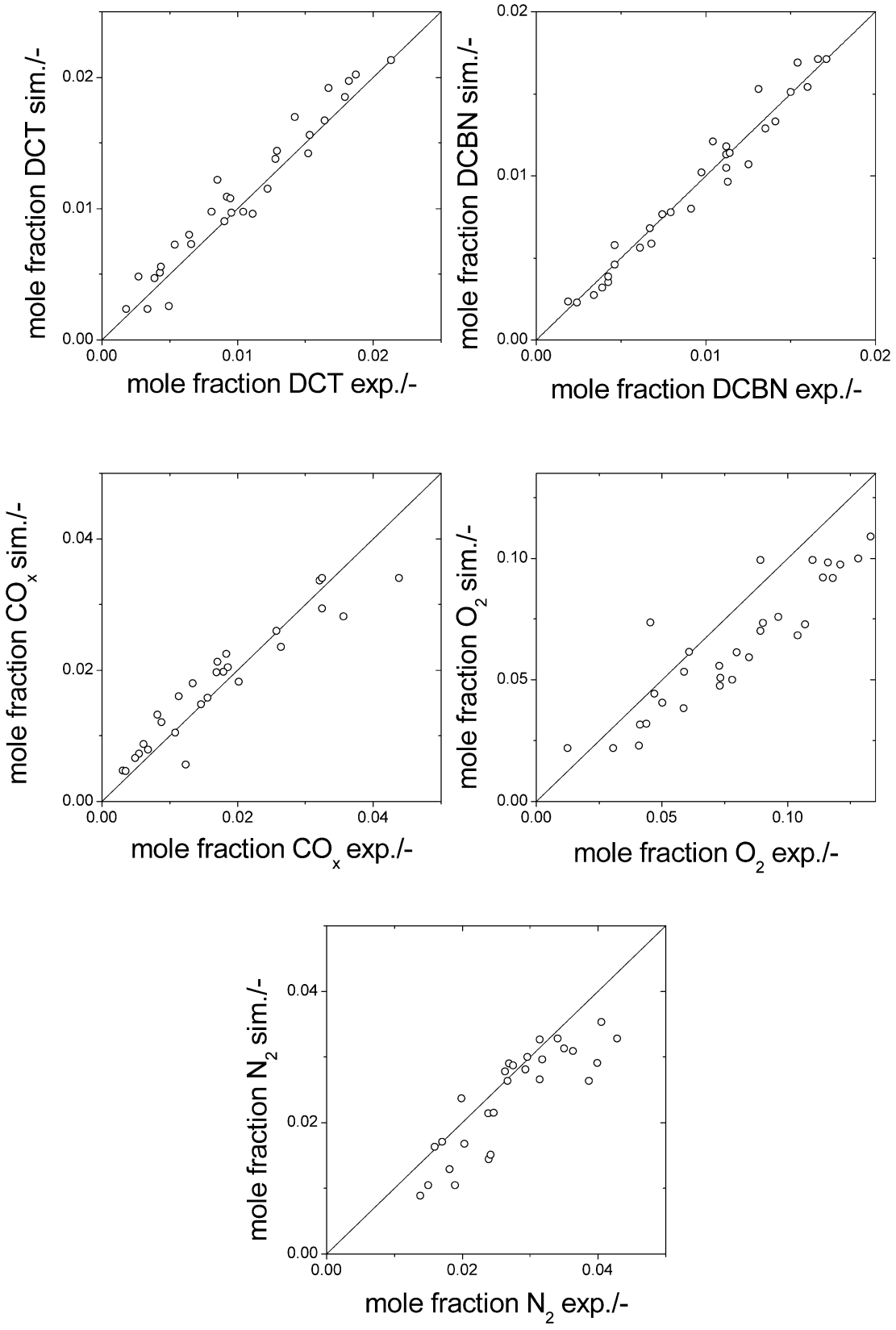

Fig. 7. Parity plots for experimental and simulated mole fractions of DCT, DCBN, CO_x, O_2 and N_2 for model with two active sites.

vanadium-containing catalysts by Prasad and Kar [26], Das and Kar [27] and Cavalli et al. [20] reporting the existence of a common adsorbed precursor or intermediate in the formation of nitrile and CO_2. Our adsorption and reaction studies of ammoxidation of toluene using infrared and pulse techniques [28,29] found complementary results on the participation of

Table 3
Experimental conditions applied in mini-plant experiments

Parameter	Case	
	A	B
Feed composition (mol%)		
DCT	2.4	2.85
Oxygen	13.2	13.2
Nitrogen[a]	53.8	29.85
Ammonia	10.6	12.0
Water	20.0	42.1
Reaction temperature (K)	653	
Pressure (bar, absolute)	1.1	
Residence time (kg_{cat} s/m^3)$_{STP}$	2200	4600

[a] In contrast to the lab scale experiments nitrogen was used as diluent.

Table 4
The comparison of experimental and simulated catalytic results obtained from gas phase ammoxidation of DCT under conditions defined in Table 3 (mini-plant)

Case	A		B	
	Simulated	Measured	Simulated	Measured
X_{DCT} (%)	85.06	78.4	98.2	100
X_{O_2} (%)	78.05	72.8	94.3	93
Y_{DCBN} (%)	65.9	61.7	76.1	83.2
Y_{CO} (%)	4.28	5.1	4.9	5.1
Y_{CO_2} (%)	14.89	12.5	17.8	11.7

lattice oxygen for selective ammoxidation reactions. In addition, temporal analysis of products experiments [29] also gave strong evidence for the insertion of nitrogen from bulk of an ammonia-containing VPO catalyst containing ^{14}N species during the initial pulses of ^{15}N containing NH_3 as a source of N-insertion for nitrile formation.

3.4. Validation of the model: Mini-plant tests

The derived kinetic model with two active sites was validated by comparing the experimental results obtained in a mini-plant unit using the up-scaled 25% VPCrO/TiO_2 catalyst with the corresponding simulation results. Experiments and simulations were carried out applying conditions given in Table 3. The temperature of the cooling media circulated in the double-walled metal oven was assumed to be constant over the reactor length and equal inlet temperature.

Mini-plant experiments were described by the pseudo-homogeneous model for a fixed-bed tubular reactor operating in the steady state with negligible axial and radial diffusion [Eqs. (1)–(4)]. The results based on the kinetic model with two active sites are presented in Table 4. The simulated values of conversions of DCT and oxygen, as well as yields of DCBN, CO, and CO_2, agree well with experimentally measured values. The small discrepancies between the simulated and experimental values of conversion and yields result from the cumulative error of the kinetic model, the activity of the up-scaled catalyst, the reactor model used for the description of the mini-plant setup, and the experimental error.

4. Conclusion

The reaction kinetics of the ammoxidation of DCT over a 25% VPCrO/TiO_2 catalyst have been studied and kinetic parameters estimated with the goal of deriving a comprehensive kinetic description of the reaction that allows simulation in a wide range of conditions. The experimental kinetic data obtained under nonisothermal conditions were correlated by the rate equations based on the Langmuir–Hinshelwood mechanism, considering competition between DCT and ammonia for the same kinds of active sites in primary ammoxidation and combustion of DCT. Another kind of active site is responsible for the combustion of ammonia to nitrogen. DCBN and carbon oxide formation exhibited approximately first-order reactions with respect to hydrocarbon partial pressure. The rates were independent of oxygen concentration when exceeding the stoichiometric amount. An inhibition effect of NH_3 on the overall DCT conversion was observed. The ammonia combustion to nitrogen exhibited a first-order reaction with respect to oxygen and was inhibited by H_2O.

The present investigation represents a first attempt to develop a mathematical model; there is ample room for improving the description of the reaction kinetics for ammoxidation of DCT in a fixed-bed reactor. Further studies are needed to clarify various aspects of this reaction for up-scaling.

Acknowledgments

Financial support provided by Tessenderlo Chemie S.A., Tessenderlo (Belgium) is gratefully acknowledged. Thanks are due to Mrs. J. Kubias and Mrs. P. Rößler for their experimental assistance. The authors also thank Dr. Q. Smejkal for his valuable discussions and cooperation in the mini-plant runs.

References

[1] A. Martin, B. Lücke, Catal. Today 57 (2000) 61.
[2] R.K. Grasselli, J.D. Burrington, in: D.D. Eley, H. Pines, P.B. Weisz (Eds.), Selective Oxidation and Ammoxidation of Propylene by Heterogeneous Catalysis, in: Advances in Catalysis, vol. 30, Academic Press, New York, 1981, p. 133.
[3] A. Martin, V.N. Kalevaru, B. Lücke, Catal. Today 78 (2003) 311.
[4] A. Martin, V.N. Kalevaru, B. Lücke, J. Sans, Green Chem. 4 (2002) 481.
[5] K.V. Narayana, A. Martin, U. Bentrup, B. Lücke, J. Sans, Appl. Catal. A 270 (2004) 57.
[6] J.N. Cosby, M. Erchak, US Patent 2,499,055 (1950), Allied Chemical and Dye corporation, New York.
[7] D.J. Hadley, Chem. Ind. (1961) 238.
[8] M. Saito, T. Okawa, Ger. Offen. Patent 2,123,836 (1970), Japan Gas Chemical Co., Tokyo.
[9] A.P. Gelbein, US Patent 3,925,447 (1974), The Lummus Company, Bloomfield, NJ.
[10] R.D. Bushick, H.P. Angstadt, US Patent 4,018,713 (1973), Sun Ventures, Inc., PA.
[11] A. Martin, B. Lücke, G.-U. Wolf, M. Meisel, Catal. Lett. 33 (1995) 349.
[12] K.V. Narayana, A. Martin, B. Lücke, M. Belmans, F. Boers, D. van Deynse, Z. Anorg. Allg. Chem. 631 (2005) 25.
[13] Z. Qiong, H. Chi, X. Guangyong, X. Chongwen, C. Yuanyin, Synth. Commun. 29 (1999) 2349.

[14] A. Martin, K.V. Narayana, B. Lücke, D. van Deynse, M. Belmans, F. Boers, WO 03/101939 A2 (2003), Tessenderlo Chemie S.A., Belgium.
[15] K. Yutaka, Y. Yasumasa, U. Masahiro, M. Hiroshi, EP Patent 0,273,317 B1 (1992), Nitto Chem. Ind. Co., Japan.
[16] Z. Qiong, H. Chi, X. Chongwen, H. Qiong, CN 1,166,378 A (1997), Wuhan Univ., China.
[17] T.H. Hayami, G.Y. Kuroda, T.M. Kikuchi, F.K. Koshi, US Patent 4,530,797 (1985), Nippon Kayaku Kabushiki Kaisha, Tokyo, Japan.
[18] M. Sanati, A. Andersson, Ind. Eng. Chem. Res. 30 (1991) 320.
[19] G. Simon, J.E. Germain, Bull. Soc. Chim. Fr. 11 (1975) 2617.
[20] P. Cavalli, F. Cavani, I. Manenti, F. Trifiro, M. El-Sawi, Ind. Eng. Chem. Res. 26 (1987) 804.
[21] A. Martin, U. Bentrup, B. Lücke, A. Brückner, Chem. Commun. (1999) 1169.
[22] P.S. van Damme, S. Narayanan, G.F. Froment, AIChE J. 21 (1975) 1065.
[23] P. Mars, D.W. van Krevelen, Chem. Eng. Sci. Special Suppl. 3 (1954) 41.
[24] G. Centi, Appl. Catal. A: Gen. 147 (1996) 267.
[25] A. Andersson, S.T. Lundin, J. Catal. 58 (1979) 383.
[26] R. Prasad, A.K. Kar, Ind. Eng. Chem. Process Des. Dev. 15 (1976) 170.
[27] A. Das, A.K. Kar, J. Chem. Technol. Biotechnol. 29 (1979) 487.
[28] Y. Zhang, A. Martin, H. Berndt, B. Lücke, M. Meisel, J. Mol. Catal. A 118 (1997) 205.
[29] A. Martin, Y. Zhang, H.W. Zanthoff, M. Meisel, M. Baerns, Appl. Catal. A: Gen. 139 (1996) L11.